



Addressing Carrier Aggregation with Narrow-band Tunable Antennas

Barrio, Samantha Caporal Del; Morris, Art; Pedersen, Gert F.

Published in:
2016 10th European Conference on Antennas and Propagation (EuCAP)

DOI (link to publication from Publisher):
[10.1109/EuCAP.2016.7481322](https://doi.org/10.1109/EuCAP.2016.7481322)

Publication date:
2016

Document Version
Accepted author manuscript, peer reviewed version

[Link to publication from Aalborg University](#)

Citation for published version (APA):
Barrio, S. C. D., Morris, A., & Pedersen, G. F. (2016). Addressing Carrier Aggregation with Narrow-band Tunable Antennas. In *2016 10th European Conference on Antennas and Propagation (EuCAP)* IEEE. <https://doi.org/10.1109/EuCAP.2016.7481322>

General rights

Copyright and moral rights for the publications made accessible in the public portal are retained by the authors and/or other copyright owners and it is a condition of accessing publications that users recognise and abide by the legal requirements associated with these rights.

- Users may download and print one copy of any publication from the public portal for the purpose of private study or research.
- You may not further distribute the material or use it for any profit-making activity or commercial gain
- You may freely distribute the URL identifying the publication in the public portal -

Take down policy

If you believe that this document breaches copyright please contact us at vbn@aub.aau.dk providing details, and we will remove access to the work immediately and investigate your claim.

Addressing Carrier Aggregation with Narrow-band Tunable Antennas

Samantha Caporal Del Barrio^{1,2}, Art Morris², Gert F. Pedersen¹,

¹Section of Antennas, Propagation and Radio Networking (APNet), Department of Electronic Systems, Faculty of Engineering and Science, Aalborg University, DK-9220, Aalborg, Denmark, scdb@es.aau.dk

²WiSpry Inc., Irvine, CA, USA

Abstract—Enhancing the operating bandwidth of antennas is particularly challenging when the antenna is confined in a very restricted volume, as is the case for mobile phones. However, increasing the bandwidth provides higher data rates to the users. Consequently, the carrier aggregation technology has been standardized. This paper proposes an antenna design that can address the bandwidth issue of new radio frequency standards, while coping with carrier aggregation requirements. Specifically, the paper presents a dual-antenna system, where each antenna exhibits a dual-resonance. The low-bands of the radio frequency spectrum can be efficiently covered.

Index Terms—4G mobile communication, Antenna measurements, Reconfigurable architectures, Mobile antennas, Multifrequency antennas, LTE communication systems.

I. INTRODUCTION

The proliferation of the Frequency Division Duplex (FDD) bands has complicated the architecture of mobile handsets. Today the frequency spectrum counts 30 FDD bands and 12 Time Division Duplex (TDD) bands worldwide, ranging from 698 MHz to 3590 MHz and from 703 MHz to 3800 MHz respectively. This is to be put in contrast with the allocation of only one tenth of these bands 10 years ago. Thus a world-wide mobile handset requires nowadays a dramatically increased front-end complexity. Indeed, while TDD operation uses a relatively simple front-end (FE) architecture, FDD operation requires one that can support simultaneous Transmitting (Tx) and Receiving (Rx) paths. On current mobile platforms, FDD operation is enabled by the use of duplex filters. However, these filters are band specific. Therefore, the FDD band proliferation has created a multiplication of the number of duplex filters needed in the mobile front-ends. Thus, in order to operate in several geographic regions, bulky and redundant architectures are implemented.

On mobile phone Printed Circuit Boards (PCBs), the real estate is highly valued and a new way of addressing the FDD band coverage is a necessity, in order to reduce the cost, volume and battery life of handsets. Several solutions have been proposed to address this issue. A comprehensive overview is given in [1]. The main approaches are:

- 1) the stacked approach [2], which stacks filters on top of the Power Amplifier (PA) in a 3D chip, which considerably reduces the space needed for the front-end but not the component count,
- 2) the division free duplex [3], where the Tx-Rx isolation is provided by a combination of signal processing and a baseband echo canceller, instead of duplex filters,
- 3) the use of the antennas as filters and the co-design of the front-end, which eliminates the need for duplex filters as well.

This paper investigates the third approach, which uses two narrow-band tunable antennas, as opposed to one typical multi-resonant antenna. These tunable antennas separately address the Tx and the Rx frequencies. Therefore, by using the duplex distance and achieving a high antenna isolation, part of the filtering is taken care of at the antenna level. The rest of the filtering can be achieved with tunable filters. As a result, the front-end does not need duplex filters anymore, which decreases considerably its complexity. Furthermore, the antennas being narrow-band, they exhibit a very low profile. This concept has been more extensively described in [1], [4], [5].

The drawback of such a dual-antenna approach is supporting carrier aggregation because of the intrinsic narrow-band nature of the system. This paper proposes an antenna design that can support intra-band and inter-band carrier aggregation with the above mentioned architecture. The paper focuses on the low-bands of the frequency spectrum, as these bands are the most challenging ones to address on small handsets.

Section II of this paper presents the antenna design while Section III discloses the simulation and measurement results. The conclusions are presented in Section IV.

II. ANTENNA DESIGN

The platform chosen to design the antennas is a typical smart-phone of dimensions 120×54 mm. The antennas are loaded with high-Q Micro-Electro-Mechanical Systems (MEMS) tunable capacitors from wiSpry [6], in order to tune their operating frequency. The antennas are narrow-band to fit the framework and allow for small elements. The Tx and the Rx antennas are independently tunable and their geometries are identical. Both the Tx and the Rx antenna exhibit a dual-resonance. Furthermore, each of the resonances of each of these antennas is independently tunable. The two resonances of each of the antennas (Tx or Rx) can also aggregate, in order to enhance their bandwidth and address the specifications of

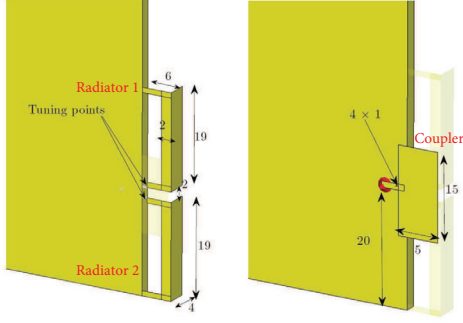


Fig. 1: Rx antenna geometry. The radiators are highlighted on the left picture and the coupler is highlighted on the right picture. The dimensions are given in mm.

carrier aggregation. Finally, the Tx and the Rx antennas are placed orthogonally in order to minimize the coupling.

A. Antenna geometry

The antenna consists of three elements: two radiators and one coupler. The geometry of the design can be seen in Fig. 1 for the Rx antenna. The drawing on the left emphasizes the dimensions of the two independently tunable radiators, whereas the drawing on the right emphasizes the dimensions of the coupler. Having two radiators is a key parameter for a carrier aggregation design. It allows to have two independent resonances that can be tuned far apart without affecting each other, or that can be joined into one wider bandwidth, in a Chebyshev-like resonance [7]. This is the main strength of the design as it allows to cope with inter-band and intra-band carrier aggregation.

The coupler is connected to the feed line. Both radiators are symmetrical and work independently. Their height and width controls the bandwidth while their length controls their natural resonance frequency. Each of the radiators is connected to a tuning point on the board. The coupler is sitting 1 mm above the radiators, and its width and length are a trade-off with the matching lumped elements that are used in the feeding circuitry. An L-match feeding network is connected to the coupler. One MEMS tuner is used at the feed. A second MEMS tuner, having two independent banks, is used on the radiators in order to handle each radiator independently. Each radiator has its own tuning point, independent from the one of the other radiator, i.e. there is no physical connection between the two radiators.

B. Mobile platform

The Tx antenna exhibits identical dimensions to the ones of the above-presented Rx antenna. It is placed on top of the board, in order to achieve high isolation between the Rx and Tx antennas. Indeed, the antennas are placed on orthogonal edges of the board to excite different modes, and interact minimally with each other [8], [9]. Both antennas (Tx and Rx) and the total volume they occupy, is represented in Fig. 2. The clearance required for each antenna is $(19 + 2 + 19) \times 6 \times (4 + 1) = 1.2 \text{ cm}^3$.

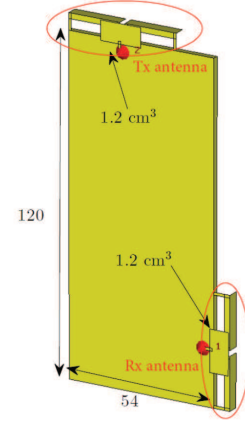


Fig. 2: Mobile platform equipped with one Tx and one Rx antenna, where each of these antennas is tunable and exhibits a dual-resonance.

C. MEMS tuners

The design presented in this paper uses 4 MEMS tuners in total, each of them exhibiting a maximum capacitance of 8 pF. Each antenna uses one tuner for the coupler and one tuner for both radiators. Both radiators can use a single tuner without being connected to each other. This is because the tuners exhibit two independent banks of 4 pF each. Each bank consists of 2 capacitors of a minimum capacitance of 0.25 pF each. The capacitance steps of the tuners is 1/16 pF, which allows for very fine antenna tuning. This is essential when addressing narrow-band antennas. The minimum capacitance of the tuners is about 1 pF.

III. SIMULATION AND MEASUREMENT RESULTS

This section presents the simulation and the measurement results of the Tx and Rx antennas in the low bands of the Long Term Evolution (LTE) frequency range [10], i.e. below 1 GHz. Firstly, the tuning range of the antennas and the feasibility of the dual-antenna (split Tx and Rx antennas) principle are investigated in III-A. Then, the carrier aggregation configurations are investigated in III-B.

A. Tuning range

To investigate the tuning range, only one radiator of each antenna is necessary. The simulation results are plotted in Fig. 3. Only the bands 5, 8, 12 and 17 are shown in the figure, in order to ease the reading. Nonetheless, the antennas can cover all the frequencies below 960 MHz until 600 MHz, while maintaining an isolation below -20 dB for the duplex spacings defined in the standard [10]. The high antenna isolation throughout tuning provides rejection between the Tx and the Rx paths.

For the sake of clarity, the band 13 is not plotted, as the Tx and Rx bands are reversed. However, the antennas can cover this band as well, as they are independently tunable. The bands at 600 MHz are included in the simulations because even though they are not part of the standard yet, they are already put for auction and will likely be added to

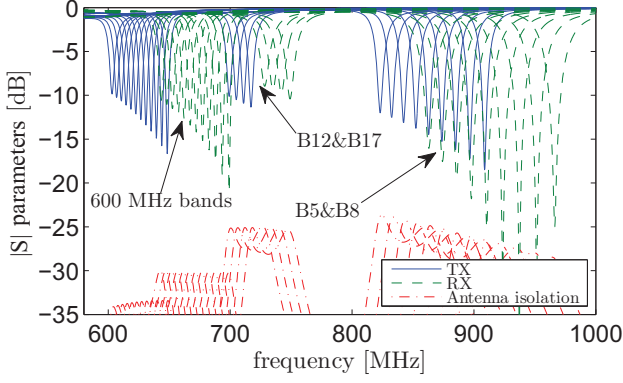


Fig. 3: Simulation results of the Rx and Tx antenna throughout tuning of the low-bands of LTE.

the LTE frequency spectrum in the near-future [11], [12]. Additionally, addressing the 600 MHz bands is a greater challenge for mobile phone antenna engineers and highlights the relevance of a new antenna-front-end paradigm, as for example the dual-antenna system presented in this paper.

Throughout tuning the obtainable bandwidth varies from 20 MHz at 960 MHz to 10 at 700 MHz and to 5 MHz at 600 MHz. The bandwidth reduction is a result of tuning, as the antenna Quality factor (Q) increases when the operating frequency is further away from the natural resonance frequency. The channel bandwidths for LTE range from 20 MHz to 1.4 MHz, depending on the operating band. Therefore, narrow channel bandwidths are valid, in the case of separated Tx and Rx antennas. Moreover, it allows the antenna to exhibit a low profile.

B. Inter-band and intra-band carrier aggregation

By using both radiators of the Tx and the Rx antennas, carrier aggregation is achieved. The authors use the bands 12 and 5 as an example for inter-band low-band carrier aggregation, as well as the bands 12 and 13 for a contiguous case. These measurements show a proof-of-concept and measurements of the full LTE carrier aggregation bands will be included in an extension of this work.

The settings on the tuners used for the inter-band aggregation of the bands 12 and 5 are summarized in Table I, the simulated $|S|$ parameters are shown in Fig. 4 and the measurements in Fig. 5. The capacitance values used in the measurements differ slightly to the ones used in the simulations and shown in Table I. This is due to the complex equivalent circuit of the MEMS tuner.

One of the strengths of this design is the independent tuning of all radiators, allowing in this example to cover bands where transmitting and receiving frequency are reversed compared to traditional bands. The settings on the tuners used for the inter-band aggregation of band 12 and 13 are summarized in Table I, the simulated $|S|$ parameters are shown in Fig. 6 and the measurements in Fig. 5. The configuration of Fig. 6 also covers band 17, as it is a subsection of band 12.

TABLE I: Capacitor values for carrier aggregation in bands 12 and 5 and in bands 12 and 13.

Bands 12 and 5	Tx Values [pF]	Rx Values [pF]
Radiator 1	2.00	1.75
Radiator 2	3.25	2.94
Bands 12 and 13	Tx Values [pF]	Rx Values [pF]
Radiator 1	2.37	2.56
Radiator 2	3.25	2.87

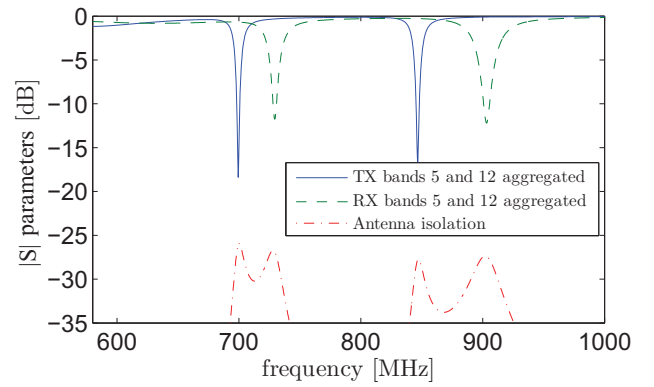


Fig. 4: Simulated $|S|$ parameters of the Tx and Rx antennas for inter-band carrier aggregation between the bands 12 and 5.

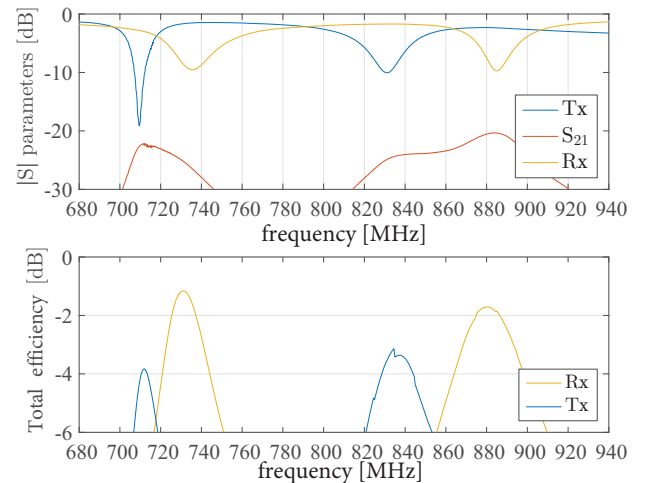


Fig. 5: Measured $|S|$ parameters and total efficiency of the Tx and Rx antennas for inter-band carrier aggregation between the bands 12 and 5 with the MEMS tuner.

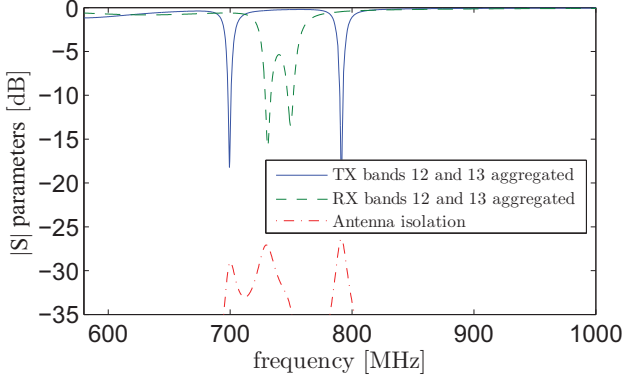


Fig. 6: Simulated $|S|$ parameters of the Tx and Rx antennas for inter-band carrier aggregation between bands 12 and 13.

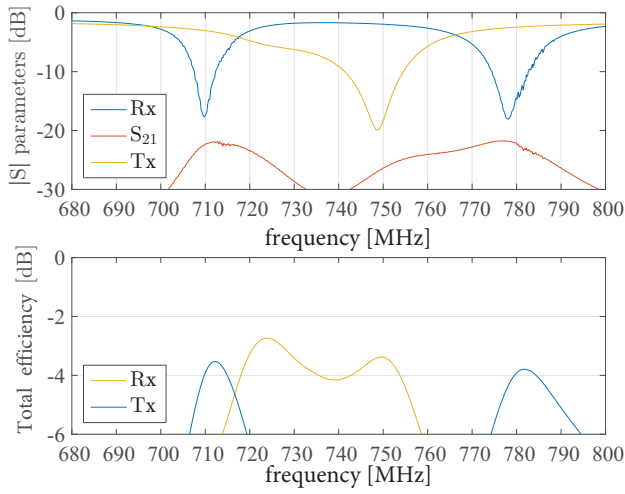


Fig. 7: Measured $|S|$ parameters and efficiency of the Tx and Rx antennas for inter-band carrier aggregation between bands 12 and 13 with the MEMS tuner.

Intra-band carrier aggregation is also achieved with the proposed design: when the resonances are brought close to each other, they join into a wider bandwidth, adopting Chebyshev like frequency response. The maximum obtainable contiguous bandwidths (intra-band contiguous aggregation) are 30 MHz at 700 MHz and 11MHz at 600 MHz.

C. Surface Currents

The surface current plots help understanding the mechanism of the proposed dual-resonant antenna design. Fig. 8 shows the Tx antenna resonating at 700 MHz when only one radiator is used, as in the tuning case shown in Fig. 3. The second radiator in that case is resonating above 1 GHz. Fig. 9 shows the surface currents on the Rx antenna at 730 MHz, when only one radiator is used as well. These shows the independence of both radiators.

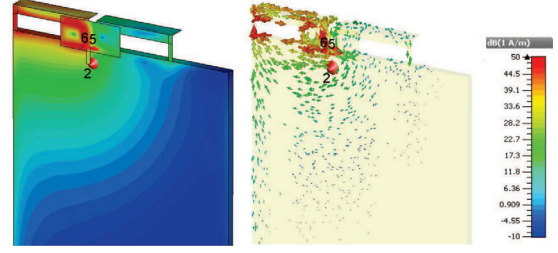


Fig. 8: Surface currents on the Tx antenna at 700 MHz.

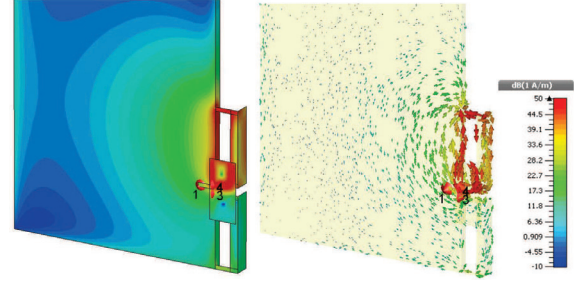


Fig. 9: Surface currents on the Rx antenna at 730 MHz.

IV. CONCLUSION

Band proliferation lead to investigating new front-end architectures enabling world-wide operation of mobile platforms. The approach of exploiting filtering antennas is limited by their intrinsic narrow-band nature. However, with a dual-resonant design, carrier aggregation can be supported by such a system. A narrow-band tunable dual-resonant antenna design is presented in this paper. Simulations and measurements exhibit the support of intra-band and inter-band carrier aggregation combinations, thus reinforcing the potential of the filtering antenna approach to resolve the bandwidth issue of newer generations of mobile communications. Measurements of the full LTE frequency spectrum will be carried out in future work, as well as voltage handling of the MEMS tuners.

ACKNOWLEDGMENT

The work is supported by the Smart Antenna Front End (SAFE) Project within the Danish National Advanced Technology Foundation - High Technology Platform.

REFERENCES

- [1] O. N. Alrabadi, A. D. Tatomirescu, M. B. Knudsen, M. Pelosi, and G. F. Pedersen, "Breaking the Transmitter-Receiver Isolation Barrier in Mobile Handsets with Spatial Duplexing," *IEEE Transactions on Antennas and Propagation*, vol. 61, no. 4, pp. 2241–2251, 2013.
- [2] Qualcomm, "Qualcomm's new radio chip gets us one step closer to a global 4G phone," 2013.
- [3] S. Chen, M. Beach, and J. McGeehan, "Division-free duplex for wireless applications," *Electronics Letters*, vol. 34, no. 2, pp. 147–148, 1998.
- [4] M. Pelosi, M. B. Knudsen, and G. F. Pedersen, "Multiple Antenna Systems with Inherently Decoupled Radiators," *IEEE Transactions on Antennas and Propagation*, vol. 60, no. 2, pp. 503–515, 2012.
- [5] S. Caporal del Barrio, A. Tatomirescu, G. F. Pedersen, and A. Morris, "Novel Architecture for LTE Worldphones," *IEEE Antennas and Wireless Propagation Letters*, vol. 12, no. 1, pp. 1676–1679, 2013.

- [6] WiSpry, "<http://www.wispri.com/products-capacitors.php>," 2014.
- [7] D. Pozar, *Microwave Engineering*. John Wiley & Sons, 4th ed., 2011.
- [8] P. Vainikainen, J. Ollikainen, O. Kivekäs, and I. Kelder, "Resonator-Based Analysis of the Combination of Mobile Handset Antenna and Chassis," *IEEE Transactions on Antennas and Propagation*, vol. 50, no. 10, pp. 1433–1444, 2002.
- [9] R. F. Harrington and J. R. Mautz, "Theory of Characteristic Modes for Conducting Bodies," *IEEE Transactions on Antennas and Propagation*, vol. 19, no. 5, pp. 622–628, 1971.
- [10] 3GPP TS 36.101, "LTE; Evolved Universal Terrestrial Radio Access (E-UTRA); User Equipment (UE) radio transmission and reception," 2013.
- [11] FierceWireless, "FCC tentatively sets March 29, 2016, as start date for 600 MHz incentive auction," 2015.
- [12] C. F. Silva, H. Alves, and A. Gomes, "Extension of LTE Operational Mode over TV White Spaces," in *Future Network and Mobile Summit*, pp. 1–13, 2011.